NASA
Technical Memorandum 107199

Army Research Laboratory
Technical Report ARL–TR–1060

An Axial-Torsional, Thermomechanical Fatigue Testing Technique

Sreeramesh Kalluri
NYMA, Inc.
Brook Park, Ohio

and

Peter J. Bonacuse
Vehicle Propulsion Directorate
U.S. Army Research Laboratory
Lewis Research Center
Cleveland, Ohio

Prepared for the
Symposium on Multiaxial Fatigue and Deformation Testing Techniques
sponsored by the American Society for Testing and Materials
Denver, Colorado, May 15, 1995

National Aeronautics and
Space Administration

DISCLAIMER NOTICE

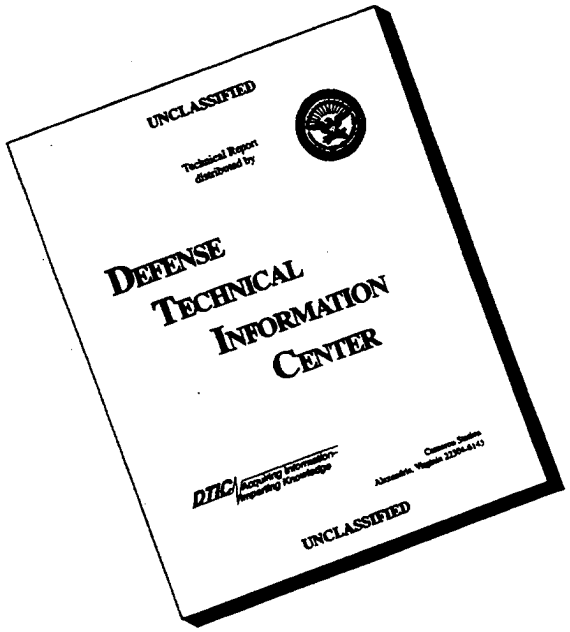

THIS DOCUMENT IS BEST QUALITY AVAILABLE. THE COPY FURNISHED TO DTIC CONTAINED A SIGNIFICANT NUMBER OF PAGES WHICH DO NOT REPRODUCE LEGIBLY.

Trade names or manufacturers' names are used in this report for identification only. This usage does not constitute an official endorsement, either expressed or implied, by the National Aeronautics and Space Administration.

AN AXIAL-TORSIONAL, THERMOMECHANICAL FATIGUE TESTING TECHNIQUE

Sreeramesh Kalluri
NYMA Inc.
Brook Park, Ohio 44142

and

Peter J. Bonacuse
Vehicle Propulsion Directorate
U.S. Army Research Laboratory
Lewis Research Center
Cleveland, Ohio 44135

ABSTRACT

A technique for conducting strain-controlled, thermomechanical, axial-torsional fatigue tests on thin-walled tubular specimens was developed. Three waveforms of loading, namely, the axial strain waveform, the engineering shear strain waveform, and the temperature waveform were required in these tests. The phasing relationships between the mechanical strain waveforms and the temperature and axial strain waveforms were used to define a set of four axial-torsional, thermomechanical fatigue (AT-TMF) tests. Real-time test control (3 channels) and data acquisition (a minimum of 7 channels) were performed with a software program written in C language and executed on a personal computer. The AT-TMF testing technique was used to investigate the axial-torsional thermomechanical fatigue behavior of a cobalt-base superalloy, Haynes 188. The maximum and minimum temperatures selected for the AT-TMF tests were 760 and 316 °C, respectively. Details of the testing system, calibration of the dynamic temperature profile of the thin-walled tubular specimen, thermal strain compensation technique, and test control and data acquisition schemes, are reported. The isothermal, axial, torsional, and in- and out-of-phase axial-torsional fatigue behaviors of Haynes 188 at 316 and 760 °C were characterized in previous investigations. The cyclic deformation and fatigue behaviors of Haynes 188 in AT-TMF tests are compared to the previously reported isothermal axial-torsional behavior of this superalloy at the maximum and minimum temperatures.

NOMENCLATURE

T	temperature
t	time
γ	engineering shear strain
ε	axial mechanical strain
λ	proportionality constant, γ_a/ε_a
ϕ	phase angle between axial mechanical and engineering shear strain waveforms
θ	phase angle between axial mechanical strain and temperature waveforms
Δ	denotes range of a variable

Subscripts:

a amplitude

min minimum value in a cycle

max maximum value in a cycle

th thermal

tot total, i.e., mechanical and thermal

INTRODUCTION

Aeronautical gas turbine and rocket engine hot section components are routinely subjected to multiaxial states of stress under nonisothermal conditions (ref. 1). The nonisothermal nature of thermal loading arises from thermal gradients generated in components such as turbine blades, combustor liners, and disks during engine start up, shutdown, and operational transients as well as from the active cooling typically used in high performance engines. Multiaxial loading arises from the thermal gradients, centrifugal and pressure loads, mechanical constraints in the components, or combinations of any of these effects. For reliable and safe operation of reusable engines, it is imperative that the deformation behavior and fatigue life of the engine components be estimated through the use of the most pertinent constitutive and life prediction models and experimental data.

Generation of cyclic deformation and fatigue life data under nonisothermal, multiaxial conditions requires development of reliable testing techniques. In particular, fatigue test definition can be complicated because of the multiaxial nature of mechanical loads and the simultaneously applied thermal load. In addition, specimen heating, test control, and data acquisition schemes must be developed to perform these complex fatigue tests.

In this paper, an experimental technique to perform nonisothermal, axial-torsional fatigue tests on thin-walled tubular specimens is described. The technique was successfully used to test tubular specimens of a cobalt-base superalloy, Haynes 188 between the temperatures of 316 and 760 °C. This material is used for the liquid oxygen carrying posts in the main injector of the reusable space shuttle main engine and for the combustor liner in the T-800 turboshaft engine for the RAH-66 Comanche helicopter. Both of these components are subjected to multiaxial stresses under nonisothermal loading conditions. Development of the test method, salient features of the testing technique, and examples of the nonisothermal, axial-torsional fatigue and deformation data are reported.

BACKGROUND

Thermomechanical Testing

Thermomechanical fatigue (TMF) tests, where a combination of both mechanical and thermal loads are typically imposed on a material specimen, have been used by designers and researchers to characterize the uniaxial, nonisothermal fatigue and deformation behaviors of reusable engine component materials (refs. 2 to 5). Over the last quarter century, several investigators developed experimental techniques to conduct TMF tests on axially loaded specimens (refs. 6 to 12). Strain-controlled axial TMF tests require active thermal strain compensation to obtain the necessary mechanical strains in a loading cycle. For a given temperature range and axial mechanical strain range, depending upon the phase difference between axial mechanical strain and temperature waveforms, an infinite number of axial strain-controlled TMF test conditions can be investigated. However, axial strain-controlled TMF tests are generally classified as either in-phase (axial tensile peak mechanical strain occurs at T_{max}; $\theta = 0^{\circ}$) or out-of-phase (axial tensile peak mechanical strain occurs at T_{min}; $\theta = 180^{\circ}$).

Thermomechanical testing under torsion was conducted by Bakis et al. (ref. 13) to investigate the cyclic deformation behavior of the nickel-base superalloy, Hastelloy X. In torsional thermomechanical testing, the active thermal strain compensation that is required in the axial thermomechanical testing is ideally not necessary. In torsional TMF tests in-phase and out-of-phase tests can be defined in a sense similar to the axial TMF tests. In general, the phase

difference between a single mechanical strain waveform and the temperature waveform is controlled in these TMF tests. Note that in axial or torsional TMF tests, the terms "in-phase" and "out-of-phase" refer to thermal phasing between either the axial mechanical strain waveform or the engineering shear strain waveform and the temperature waveform.

Axial-Torsional Testing

Fatigue testing under combined axial-torsional loading is routinely conducted on thin-walled tubular specimens under isothermal conditions. Over the past twenty years, several researchers have developed testing facilities and techniques to conduct isothermal, axial-torsional tests at both room and elevated temperatures (refs. 14 to 20). As in axial or torsional TMF testing, for a given set of axial and engineering shear strain ranges, an infinite number of combined axial-torsional loading conditions can be investigated depending upon the phase difference between the axial and engineering shear strain waveforms. The combined axial-torsional fatigue tests are commonly classified as in-phase or proportional loading (axial strain peak and engineering shear strain peak occur at the same time; $\phi = 0^\circ$) or out-of-phase or nonproportional loading (axial strain peak leads the engineering shear strain peak by a quarter of a waveform; $\phi = 90^\circ$). In combined axial-torsional fatigue tests, the terms "in-phase" and "out-of-phase" refer to mechanical phasing between the axial and engineering shear strain waveforms.

Note that the terms "in-phase" and "out-of-phase" as used in the literature for axial TMF tests and isothermal, combined axial-torsional fatigue tests have two significant differences. First, as mentioned earlier, these terms represent thermal phasing in axial TMF tests, whereas they represent mechanical phasing in isothermal, combined axial-torsional fatigue tests. Second, an out-of-phase test typically denotes a phase angle, $\theta = 180^\circ$ in the axial TMF tests, whereas it commonly denotes a phase angle, $\phi = 90^\circ$ in isothermal, combined axial-torsional fatigue tests.

AXIAL-TORSIONAL, THERMOMECHANICAL FATIGUE (AT-TMF) TESTING

Thermomechanical tests under combined axial-torsional loading require the control of three waveforms of loading (temperature, axial strain, and engineering shear strain) and two types of phase differences: (1) a thermal phasing as in axial TMF tests and (2) a mechanical phasing between the axial and the engineering shear strain waveforms. An infinite number of AT-TMF test conditions are possible, depending upon the combinations of mechanical and thermal phasings. In this paper, four types of AT-TMF tests are conceived by permutating the commonly investigated thermal ($\theta = 0^\circ$ and 180°) and mechanical ($\phi = 0^\circ$ and 90°) phasings in axial TMF and isothermal, combined axial-torsional fatigue tests, respectively. The AT-TMF tests are defined as follows: (1) Mechanically In-phase and Thermally In-phase (MIPTIP) test, $\phi = \theta = 0^\circ$; (2) Mechanically In-phase and Thermally Out-of-Phase (MIPTOP) test, $\phi = 0^\circ$ and $\theta = 180^\circ$; (3) Mechanically Out-of-Phase and Thermally In-Phase (MOPTIP) test, $\phi = 90^\circ$ and $\theta = 0^\circ$; and (4) Mechanically Out-of-Phase and Thermally Out-of-Phase (MOPTOP) test, $\phi = 90^\circ$ and $\theta = 180^\circ$. Note that both the "thermal phasing" and the "mechanical phasing" are referred to as either "in-phase" or "out-of-phase" depending upon the temperature waveform (for "thermal") and engineering shear strain waveform (for "mechanical") relationships to the axial strain waveform. Schematic axial mechanical strain, engineering shear strain, and temperature waveforms with appropriate phasings are shown in figure 1 for all four types of AT-TMF tests. In figures 1(a) to (d), points A and C identify the locations of maximum and minimum temperatures in a cycle, respectively, and points B and D identify the locations of intermediate points, where the mean temperature occurs in a cycle.

In this study, all four types of AT-TMF tests were conducted on thin-walled tubular specimens of Haynes 188 superalloy between the temperatures of 316 and 760 °C. The selection of the maximum and minimum temperatures for the AT-TMF program was governed by the following: (1) Haynes 188 exhibits a ductility minimum at 760 °C (ref. 21), which can significantly influence the low-cycle fatigue life, and (2) the isothermal, axial ($\lambda = 0$), torsional ($\lambda = \infty$), and combined mechanically in- and out-of-phase axial-torsional ($\lambda = 1.73$; $\phi = 0$ and 90°, respectively) fatigue experiments were previously conducted at 316 and 760 °C on the same heat of Haynes 188. The fatigue and cyclic deformation data and applicability of different multiaxial fatigue life prediction models to the isothermal, axial-torsional data of Haynes 188 were reported in references 22 to 25.

EXPERIMENTAL DETAILS

Materials and Specimens

Solution-annealed, hot rolled, and centerless ground, 50.8 mm diameter round bars of wrought Haynes 188 superalloy were supplied by a commercial vendor. The chemical composition of the superalloy in weight percent is as follows: <0.002 S, 0.002 B, 0.012 P, 0.1 C, 0.4 Si, 0.034 La, 0.75 Mn, 1.24 Fe, 13.95 W, 21.84 Cr, 22.43 Ni, with the balance being cobalt. Thin-walled tubular test specimens (fig. 2) were machined from these round bars. The bore of every tubular specimen was finished by a honing operation. Further details on machining of tubular specimens are available in ref. 26.

Test system

The AT-TMF test system consisted of an axial-torsional load frame with a capacity of ±223 kN axially and ±2.26 kN-m in torsion. The load frame was controlled with dual servocontrollers, one each for the axial and torsional actuators. A schematic of the AT-TMF test system is shown in figure 3. Axial and engineering shear strains were measured and controlled with a commercially available, water-cooled, axial-torsional extensometer equipped with quartz probes. Two indentations, 25 mm apart (gage section) and 80 μm deep, were pressed into the outer surface of every tubular specimen to mount the quartz probes of the extensometer. A photograph of the axial-torsional extensometer mounted on a calibration fixture is shown in figure 4. Specimens were heated in a three-coil (each coil is independently movable) heating fixture (ref. 27) connected to a 50 kW audio frequency induction heating unit. The number of turns in the top, middle, and bottom coils were five, one, and five, respectively.

Test control and data acquisition were performed with a computer system equipped with digital to analog and analog to digital converters and interfaced with the servocontrollers, the temperature controller, and the temperature measuring instruments. Specifications of the computer system and test interface hardware are listed in table I. Interrupt driven software for conducting the tests was written in C language. Three command waveforms (ε, γ, and T) were generated and data from 11 channels (axial and torsional loads, strains, and strokes, and temperatures at five locations on the specimen) were acquired at a rate of 1000 points/cycle. The software provided a keyboard interruption capability and a graphical display of axial and shear stresses versus time, data from the temperature measuring instruments, and test status.

Temperature Measurement and Control

Prior to the AT-TMF testing program, configuration of the three coils in the induction heating fixture was determined through the use of an axial-torsional specimen with 16 chromel-alumel thermocouples spot-welded to locations illustrated in figure 5. This heavily thermocoupled specimen was dedicated for temperature measurement along the straight section of the specimen and for establishing the individual locations of the three coils in the heating fixture. The thermocouple layout shown in figure 5 is not suitable for conducting fatigue tests because fatigue cracks can initiate from the thermocouple spot-welds in the straight section, which includes the gage section, of the specimen. If the temperature in the gage section of the specimen can be monitored separately, thermocouples can be mounted in the shoulder regions of the specimen to control the temperature during a fatigue test. In a study involving axial thermomechanical deformation tests on tubular specimens of Hastelloy X, Castelli and Ellis (ref. 11) reported that lack of adequate control of temperature profile in the straight section of the specimen resulted in cycle-dependent barrelling of the specimens. In an attempt to inhibit the cycle-dependent geometric instabilities in the AT-TMF tests, the coil configuration in the induction heating fixture was optimized by minimizing the thermal gradients in the straight section of a thermocoupled axial-torsional specimen (fig. 5) at T_{max} under dynamic conditions. The maximum allowable temperature deviation in the straight section at T_{max} under dynamic conditions was no more than 1 percent of T_{max}. For a temperature range of 316 to 760 °C, this temperature criterion under dynamic conditions was satisfied with a cycle time of 10 min.

In the AT-TMF tests, the temperature in the gage section of the tubular specimens was measured with a noncontacting optical system equipped with a sapphire probe. Four thermocouples, two each in the top and bottom shoulder regions, were spot-welded to the specimen. The specimen temperature was controlled with one of the two

thermocouples spot-welded in the top shoulder region of the specimen, where the total movement of the specimen is considerably smaller compared to the bottom shoulder region of the specimen. The cycle time (10 min) of the AT-TMF tests was dictated by the ability to obtain an acceptable gage section temperature under dynamic conditions over the temperature range of 316 to 760 °C.

In each AT-TMF test, the remote location temperature control waveform required to achieve the acceptable gage section temperature waveform was obtained by a real-time, successive-correction, training method (fig. 6). The training was conducted under load control near zero axial and torsional loads. Initially a temperature control waveform was assumed for the remote location and three thermal cycles were applied to allow the specimen to reach dynamic equilibrium. The corresponding gage section temperature waveform from the last of these three cycles was stored. In each training cycle, the procedure involved modification of the previously stored remote location temperature control waveform by operating on the difference between the desired and the real-time gage section temperature waveforms. The training method was terminated when the largest deviation of the actual temperature in the gage section of the specimen was no more than 6 °C from the desired temperature at each point in a cycle. Typically about 6 to 12 iterations (or thermal cycles) were required for this training. An example of the gage section temperature achieved after training the remote location temperature control waveform is shown in figure 7. After terminating the temperature training, axial thermal strain versus temperature data from the next five cycles were acquired. Two sixth order polynomial fits, one for heat up from 316 to 760 °C and another for cool down from 760 to 316 °C, were derived from the data using least squares analyses. These polynomials were subsequently used to calculate axial thermal strain compensation values during the AT-TMF test.

Axial thermal strain compensation

Real-time, thermal strain compensation is necessary in axial and axial-torsional TMF tests to impose the required mechanical axial strain range on the test specimens. A method to verify the validity of thermal strain compensation technique involves starting the TMF test under strain control with $\varepsilon_{max} = \varepsilon_{min} = 0$ and monitoring the axial stresses developed in the specimen (ref. 11). If the axial stresses developed in the specimen are sufficiently small in comparison to the magnitudes of the maximum and minimum stresses developed in the actual TMF test then thermal strain compensation is acceptable. In the case of AT-TMF tests, the functional relations established after the temperature training, between temperature and thermal strain for the heat up and cool down portions of the cycle, and real-time temperatures were used to offset the thermal strains. Axial stresses developed under strain control in one of the AT-TMF tests (largest in magnitude, i.e., worst case) during a thermal cycle (with $\varepsilon_{max} = \varepsilon_{min} = \gamma_{max} = \gamma_{min} = 0$) leading to the fatigue part of the AT-TMF test are shown in figure 8. The magnitude of the largest axial stress developed during the temperature cycle was about 14 MPa, which indicated that the axial thermal strain compensation technique was functioning adequately.

Fatigue Test procedure

Total axial strain control values for the AT-TMF tests were obtained by using the following equation.

$$\varepsilon_{tot}(t) = \varepsilon_{th}\left(F[T(t)]\right) + \varepsilon(t) \tag{1}$$

In this equation appropriate functions F[T(t)], determined after terminating the temperature training procedure with least squares analyses for the heat up and cool down portions of the cycle, were used for ε_{th}. In calculating the strains and stresses, the software accounted for the continuous change in the gage length and other geometric parameters of the specimen, which resulted from the changing temperature in the AT-TMF cycle. A flow chart illustrating the procedure followed for conducting AT-TMF tests is shown in figure 9. Each AT-TMF test was started in load control, and the specimen was heated to the mean temperature of 538 °C and stabilized at this temperature for 45 min to an hour. After initializing the hardware and software, the servocontrollers were switched to strain control and the temperature was cycled between 760 and 316 °C for three cycles to achieve dynamic equilibrium. During these cycles axial stress data were acquired to verify the thermal strain compensation technique. After creating the required thermal and mechanical phase shifts, the AT-TMF cycling of the specimen was started. During the test, axial stresses, strains, and stroke values, shear stresses (obtained by assuming a uniform distribution through the thin

wall of the tubular specimen), engineering shear strains, and torsional stroke values in a cycle, and the associated cycle number were acquired at logarithmic intervals. The AT-TMF test was terminated when a load drop of 5 to 10 percent was detected in either the axial or torsional peak loads as compared to a previously recorded cycle.

AT-TMF TEST RESULTS

Four strain-controlled AT-TMF tests (one each of MIPTIP, MIPTOP, MOPTIP, and MOPTOP) were conducted with $\Delta\varepsilon = 0.08$, $\Delta\gamma = 0.014$, and $\lambda = 1.75$ between the temperatures of 316 and 760 °C. In all the tests, fatigue cracks that caused failure initiated in the gage section of the specimen. Upon further examination of the failed specimens, a small amount of barrelling was observed outside the gage section of the MOPTOP test specimen. No barrelling was observed in the other three types of AT-TMF test specimens. In the following sections data generated in the AT-TMF tests are presented.

Hysteresis loops

The hysteresis loops generated in two of the AT-TMF tests are shown in figure 10. In this figure, axial and torsional hysteresis loops for cycles 2 (the first fully developed cycle), 10, and 50 are shown along with the temperature identifiers A, B, C, and D. For all the hysteresis loops in Fig. 10, points A through D correspond to the similarly identified points in figure 1. In the MIPTIP test (fig. 10(a)), both the axial and torsional hysteresis loops indicated rapid hardening in Haynes 188, particularly at the cold end of the cycle (point C). In the 10th and 50th cycles, both the axial and torsional hysteresis loops exhibited stress relaxation near the maximum temperature of the cycle (point A). The hysteresis loops from the MIPTOP test were similar to those observed in the MIPTIP test, except that the stress relaxation in MIPTOP test occurred on the negative side of the stress axis for both axial and torsional hysteresis loops. Hysteresis loops from the MOPTOP test (fig. 10(b)) were different from those observed in the mechanically in-phase MIPTIP and MIPTOP tests, which clearly indicated the influence of mechanical phasing in AT-TMF tests. Hysteresis loops from the MOPTIP test were similar to those observed in the MOPTOP test, except that the stress relaxation occurred on the positive side of the stress axis for both axial and torsional hysteresis loops.

Fatigue lives

Fatigue lives observed in the AT-TMF tests are compared in figure 11 to those reported previously for the isothermal, axial-torsional fatigue tests under similar axial and engineering shear strain ranges (refs. 22 and 24). Under mechanically in- and out-of-phase conditions, the isothermal fatigue lives at 760 °C were lower than the corresponding isothermal fatigue lives at 316 °C. This is because the ductility of Haynes 188 at 760 °C, where it exhibits a minimum, is lower than that at 316 °C. Fatigue lives of the thermally in-phase MIPTIP and MOPTIP tests were lower than the corresponding isothermal fatigue lives at 760 °C by factors of 3 to 4. This observation suggests that isothermal, axial-torsional fatigue test data generated at the maximum temperature of the cycle, do not capture the synergistic damage mechanisms precipitating under nonisothermal, axial-torsional loading conditions. Fatigue lives of the thermally out-of-phase MIPTOP and MOPTOP tests were not significantly lower than the corresponding isothermal fatigue lives at 760 °C.

Cyclic hardening

Evolution of the axial and shear stresses observed in the mechanically out-of-phase AT-TMF tests are compared in figure 12 with the cyclic hardening data generated at the same strain ranges in previous programs on isothermal, axial-torsional fatigue (refs. 22 to 24). Axial stresses exhibited pronounced cyclic hardening under thermomechanical conditions (fig. 12(a)), particularly near the cold end of the cycle, as compared to the isothermal data. Significantly higher cyclic hardening was also observed in shear stresses under thermomechanical conditions compared to the isothermal conditions (fig. 12(b)). These two observations suggest that mechanisms of deformation activated under thermomechanical loading can be distinctly different from those activated under isothermal, axial-torsional loading.

DISCUSSION

In the AT-TMF tests the cycle time was dictated by the ability to obtain an acceptable dynamic temperature waveform in the gage section. The cycle time of 10 min used in this investigation was required because of the large size of the tubular specimen and was dictated by the natural cooling rate at the low temperature end of the cycle. If nonisothermal, axial-torsional fatigue tests need to be conducted at smaller axial and engineering shear strain ranges (i.e., to obtain longer cyclic lives) then such a large cycle time may be impractical. Under these circumstances forced cooling of the specimen by compressed air blown either through the bore of the specimen or on the external surfaces of the specimen can reduce the cycle time for conducting AT-TMF tests. A smaller temperature range, $(T_{max} - T_{min})$ can also reduce the cycle time of the AT-TMF tests.

The small amount of barrelling observed beyond the gage section in the MOPTOP test could be the result of a local hot zone in the straight section of the specimen. This phenomenon may not have affected the fatigue life in a significant manner. However, duplication of the MOPTOP test can ascertain whether (1) the small amount of observed barrelling recurs and (2) whether fatigue life is affected by this phenomenon. If barrelling recurs then the dynamic temperature waveforms beyond the gage section of the specimen should also be included in the temperature training scheme.

In the MIPTIP test, the stress relaxation became more pronounced with the number of applied cycles in the axial and torsional hysteresis loops (figs. 10(a)) near the hot end of the cycle. The second cycle axial hysteresis loop did not exhibit any stress relaxation behavior because the magnitude of the stress was small. However, after a few cycles the material hardened, and the magnitude of the stress was large enough for the onset of stress relaxation. In the mechanically in-phase MIPTIP and MIPTOP tests, strain hardening occurred near the cold end of the cycle, whereas thermal recovery occurred at the hot end of the cycle. In the MOPTOP test (figs. 10(b)), which exhibited more hardening than the MIPTIP test, a small amount of stress relaxation was present even in the second cycle axial hysteresis loop. Stress relaxation was observed predominantly in the axial hysteresis loops in the mechanically out-of-phase MOPTIP and MOPTOP tests. This is because in the torsional hysteresis loops maximum temperature occurred at much lower magnitudes of shear stresses in the mechanically out-of-phase tests compared to the mechanically in-phase tests.

In this investigation, one test was conducted for each of the four defined AT-TMF tests. Duplication of these tests is necessary to assess scatter in the fatigue data. The technique proposed in this paper can be used to conduct AT-TMF tests with different maximum and minimum temperatures on Haynes 188 or other materials. The cyclic deformation and fatigue data generated with this technique would be useful either to validate existing constitutive and fatigue life prediction models or to develop improved models.

CONCLUSIONS

A technique to perform axial-torsional, thermomechanical fatigue (AT-TMF) tests was developed and the following four types of tests were defined. They are, (1) Mechanically in-phase and thermally in-phase (MIPTIP) test, (2) Mechanically in-phase and thermally out-of-phase (MIPTOP) test, (3) Mechanically out-of-phase and thermally in-phase (MOPTIP) test, and 4) Mechanically out-of-phase and thermally out-of-phase (MOPTOP) test. A computer program was developed for test control and data acquisition in real-time from the AT-TMF tests. Axial-torsional, thermomechanical fatigue tests were conducted on thin-walled tubular specimens of a wrought, cobalt-base superalloy, Haynes 188 between the temperatures of 316 and 760 °C. The following conclusions are drawn from the study.

(1) Shapes of the axial and torsional hysteresis loops were strongly influenced by the mechanical phasing in the AT-TMF tests. The location and extent of stress relaxation in the axial and torsional hysteresis loops were strongly dictated by the thermal phasing in the AT-TMF tests.

(2) Fatigue lives of the thermally in-phase AT-TMF tests were lower than the corresponding isothermal fatigue lives at 760 °C by factors of 3 to 4 indicating that isothermal, axial-torsional fatigue test data generated at the maximum temperature of the cycle can not provide a lower bound on fatigue life for the design of structural components subjected to thermally in-phase biaxial loading conditions. Fatigue lives of the thermally out-of-phase MIPTOP and MOPTOP tests, were not significantly lower than the corresponding isothermal fatigue lives at 760 °C.

(3) The rates of cyclic hardening observed (in both the axial and shear stresses) during the AT-TMF tests were much higher than those observed in isothermal axial-torsional tests at 316 and 760 °C.

(4) The axial-torsional, thermomechanical fatigue testing technique reported in this paper can be used to generate cyclic deformation and fatigue data for validation of existing constitutive and fatigue life prediction models under nonisothermal, multiaxial loading conditions.

ACKNOWLEDGMENT

The valuable technical discussions with Mr. Mike Castelli (NYMA, Inc.) and Mr. Mike Verrilli (NASA-Lewis Research Center) during the development of the testing technique, the steadfast encouragement from Mr. Rod Ellis (NASA-Lewis Research Center) throughout this program, and the technical assistance provided by Mr. Chris Burke (NYMA, Inc.) in the High Temperature Fatigue and Structures Laboratory, NASA-Lewis Research Center, are gratefully acknowledged.

REFERENCES

1. Leese, G.E. and Bill, R.C., "Multiaxial and Thermomechanical Considerations in Damage Tolerant Design," Damage Tolerance Concepts for Critical Engine Components, AGARD-CP-393, Presented at the 60th Meeting of Structures and Materials Panel, San Antonio, Texas, 1985, pp. 15–1 to 15–13.
2. Bill, R.C., Verrilli, M.J., McGaw, M.A., and Halford, G.R., "Preliminary Study of Thermomechanical Fatigue of Polycrystalline Mar-M 200," NASA TP–2280, AVSCOM TR 83-C-6, National Aeronautics and Space Administration, Washington, DC, February, 1984.
3. Marchand, N., L'Esperance, G., and Pelloux, R.M., "Thermal-Mechanical Cyclic Stress-Strain Responses of Cast B-1900+Hf," Low Cycle Fatigue, ASTM STP 942, H.D. Soloman, G.R. Halford, L.R. Kaisand, and B.N. Leis, Eds., American Society for Testing and Materials, Philadelphia, 1988, pp. 638–656.
4. Cook, T.S., Kim, K.S., and McKnight, R.L., "Thermal Mechanical Fatigue of Cast Rene 80," Low Cycle Fatigue, ASTM STP 942, H.D. Soloman, G.R. Halford, L.R. Kaisand, and B.N. Leis, Eds., American Society for Testing and Materials, Philadelphia, 1988, pp. 692–708.
5. Castelli, M.G., Miner, R.V., and Robinson, D.N., "Thermomechanical Deformation Behavior of a Dynamic Strain Ageing Alloy, Hastelloy X," Thermomechanical Fatigue Behavior of Materials, ASTM STP 1186, H. Sehitoglu, Ed., American Society for Testing and Materials, Philadelphia, 1993, pp. 106–125.
6. Carden, A.E. and Slade, T.B., "High-Temperature Low-Cycle Fatigue Experiments on Hastelloy X," Fatigue at High Temperature, ASTM STP 459, American Society for Testing and Materials, Philadelphia, 1969, pp. 111–129.
7. Carden, A.E., "Thermal Fatigue Evaluation," Manual on Low Cycle Fatigue Testing, ASTM STP 465, American Society for Testing and Materials, Philadelphia, 1970, pp. 163–188.
8. Hopkins, S.W., "Low-Cycle Thermal Mechanical Fatigue Testing," Thermal Fatigue of Materials and Components, ASTM 612, D. A. Spera and D. F. Mowbray, Eds., American Society for Testing and Materials, Philadelphia, 1976, pp. 157–169.
9. Jaske, C.E., "Thermal-Mechanical, Low-Cycle Fatigue of AISI 1010 Steel," Thermal Fatigue of Materials and Components, ASTM 612, D.A. Spera and D.F. Mowbray, Eds., American Society for Testing and Materials, Philadelphia, 1976, pp. 170–198.
10. Malpertu, J.L., and Remy, L., "Thermomechanical Fatigue Behavior of a Superalloy," Low Cycle Fatigue, ASTM STP 942, H.D. Soloman, G.R. Halford, L.R. Kaisand, and B.N. Leis, Eds., American Society for Testing and Materials, Philadelphia, 1988, pp. 657–671.
11. Castelli, M.G., and Ellis, J.R., "Improved Techniques for Thermomechanical Testing in Support of Deformation Modeling," Thermomechanical Fatigue Behavior of Materials, ASTM STP 1186, H. Sehitoglu, Ed., American Society for Testing and Materials, Philadelphia, 1993, pp. 195–211.
12. Koster, A., Fleury, E., Vasseur, E. and Remy, L., "Thermal-Mechanical Fatigue Testing," Automation in Fatigue and Fracture: Testing and Analysis, ASTM 1231, C. Amzallag, Ed., American Society for Testing and Materials, Philadelphia, 1994, pp. 563–580.
13. Bakis, C.E., Castelli, M.G., and Ellis, J.R., "Thermomechanical Testing in Torsion: Test Control and Deformation Behavior," Advances in Multiaxial Fatigue, STP 1191, D.L. McDowell and J.R. Ellis, Eds., American Society for Testing and Materials, Philadelphia, 1993, pp. 223–243.

14. Blass, J.J., and Zamrik, S.Y., "Multiaxial Low-Cycle Fatigue of Type 304 Stainless Steel," ASME-MPC Symposium on Creep-Fatigue Interaction, MPC-3, R.M. Curran Ed., The American Society of Mechanical Engineers, New York, December 1976, pp. 129–159.
15. Kanazawa, K., Miller, K.J., and Brown, M.W., "Low-Cycle Fatigue Under Out-of-Phase Loading Conditions," Journal of Engineering Materials and Technology, July 1977, pp. 222–228.
16. Socie, D.F., Waill, L.A., and Dittmer, D.F., "Biaxial Fatigue of Inconel 718 Including Mean Stress Effects," Multiaxial Fatigue, ASTM STP 853, K. J. Miller and M. W. Brown, Eds., American Society for Testing and Materials, Philadelphia, 1985, pp. 463–481.
17. Fatemi, A., and Stephens, R.I., "Biaxial Fatigue of 1045 Steel Under In-Phase and 90 Deg Out-of-Phase Loading Conditions," Multiaxial Fatigue: Analysis and Experiments, AE-14, G.E. Leese and D. Socie, Eds., Society of Automotive Engineers, Warrendale, PA, 1989, pp. 121–138.
18. Jayaraman, N., and Ditmars, M.M., "Torsional and Biaxial (Tension-Torsion) Fatigue Damage Mechanisms in Waspaloy at Room Temperature," International Journal of Fatigue, 11, No. 5, 1989, pp. 309–318.
19. Fernando, U.S., Miller, K.J., and Brown, M.W., "Computer Aided Multiaxial Fatigue Testing," Fatigue and Fracture of Engineering Materials and Structures, Vol . 13, No. 4, 1990, pp. 387–398.
20. Kalluri, S. and Bonacuse, P.J., "A Data Acquisition and Control Program for Axial-Torsional Fatigue Testing," Applications of Automation Technology to Fatigue and Fracture Testing, ASTM STP 1092, A.A. Braun, N.E. Ashbaugh, and F.M. Smith Eds., American Society for Testing and Materials, Philadelphia, 1990, pp. 269–287.
21. Nickel Base Alloys, International Nickel Company, Inc., New York, 1977.
22. Kalluri, S. and Bonacuse, . J., "In-Phase and Out-of-Phase Axial-Torsional Fatigue Behavior of Haynes 188 Superalloy at 760°C," Advances in Multiaxial Fatigue, ASTM STP 1191, D.L. McDowell and J.R. Ellis, Eds., American Society for Testing and Materials, Philadelphia, 1993, pp. 133–150.
23. Bonacuse, P.J. and Kalluri, S., "Cyclic Axial-Torsional Deformation Behavior of a Cobalt-Base Superalloy," Cyclic Deformation, Fracture, and Nondestructive Evaluation of Advanced Materials: Second Volume, ASTM STP 1184, M.R. Mitchell and O. Buck, Eds., American Society for Testing and Materials, Philadelphia, 1994, pp. 204–229.
24. Kalluri, S., and Bonacuse, P.J., "Estimation of Fatigue Life under Axial-Torsional Loading," Material Durability/Life Prediction Modeling: Materials for the 21st Century, PVP-Vol. 290, S.Y. Zamrik and G.R. Halford, Eds., American Society of Mechanical Engineers, 1994, pp. 17–33.
25. Bonacuse, P.J. and Kalluri, S., "Elevated Temperature Axial and Torsional Fatigue Behavior of Haynes 188," Journal of Engineering Materials and Technology, Vol. 117, April 1995, pp. 191–199.
26. Bonacuse, P.J. and Kalluri, S., "Axial-Torsional Fatigue: A Study of Tubular Specimen Thickness Effects," Journal of Testing and Evaluation, JTEVA, Vol. 21, No. 3, May 1993, pp. 160–167.
27. Ellis, J.R., and Bartolotta, P.A., "Adjustable Work Coil Fixture Facilitating the Use of Induction Heating in Mechanical Testing," Paper presented at the ASTM Symposium on Multiaxial Fatigue and Deformation Testing Techniques, Denver, Colorado, May 15, 1995.

TABLE I.—SPECIFICATIONS OF COMPUTER SYSTEM AND TEST INTERFACE HARDWARE

i486 Based PC-AT Compatible Computer
33 MHz Clock Speed
16 MB RAM
100 MB Hard Disk
1.2 MB and 1.44 MB Floppy Drives
Digital to Analog Converters
16 bit Resolution, 2 Channels
12 bit Resolution, 2 Channels
Analog to Digital Converters
16 bit Resolution, 8 Channel Differential Input
12 bit Resolution, 8 Channel Low-Voltage Differential Input

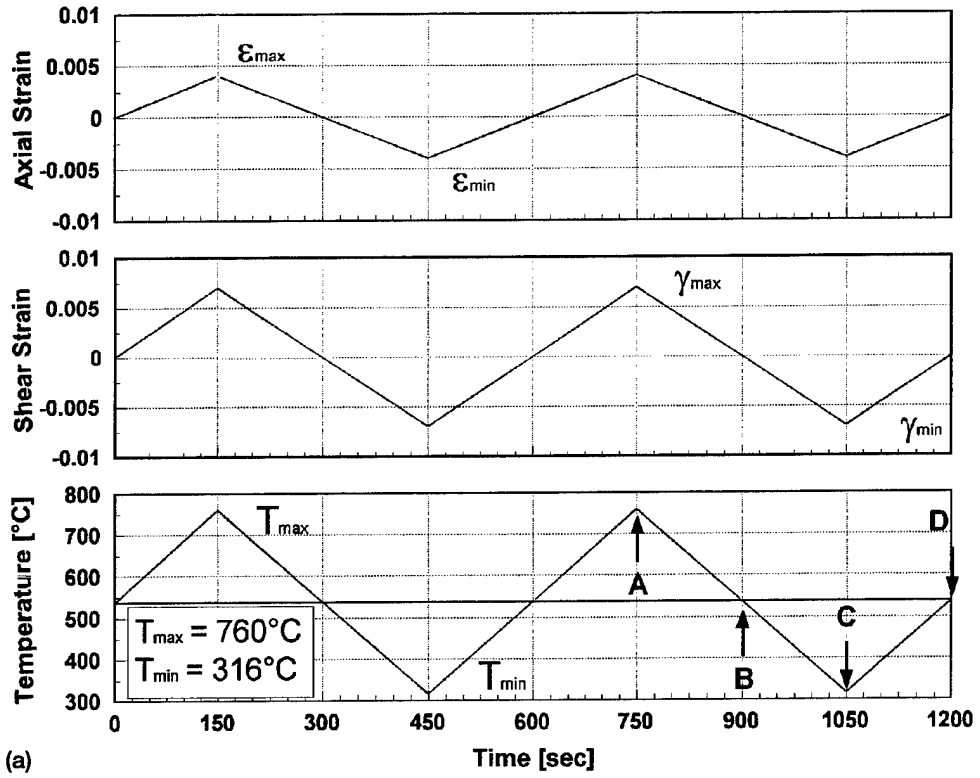

(a)

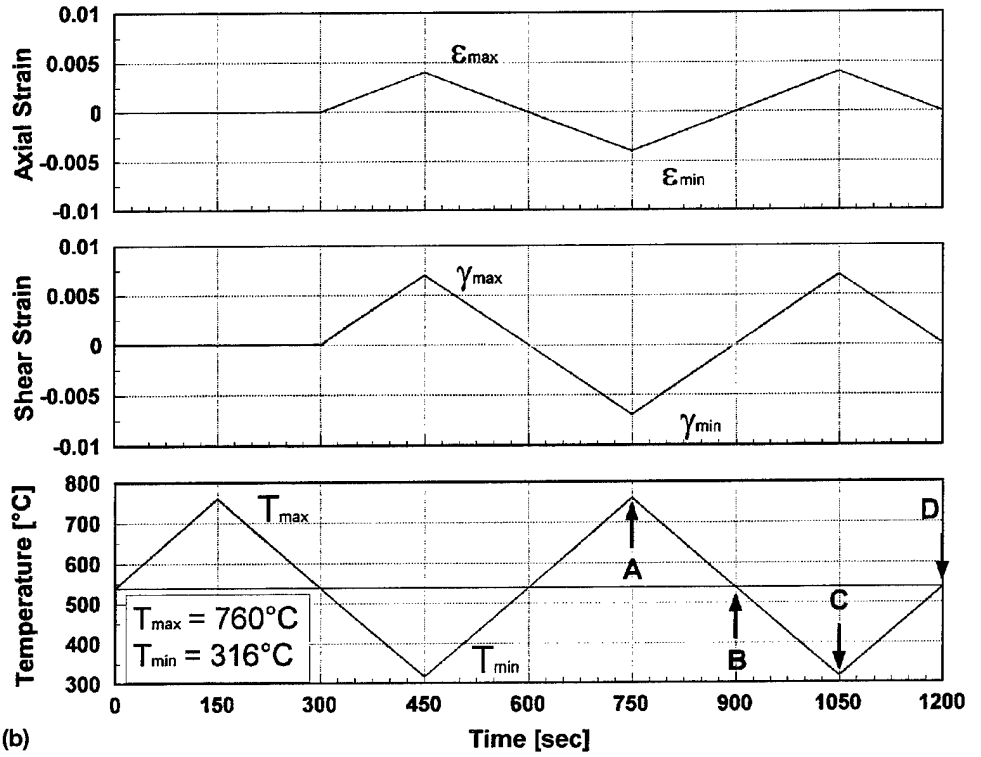

(b)

Figure 1.—Schematic axial mechanical strain, engineering shear strain, and temperature waveforms for AT-TMF tests. (a) MIPTIP test. (b) MIPTOP test.

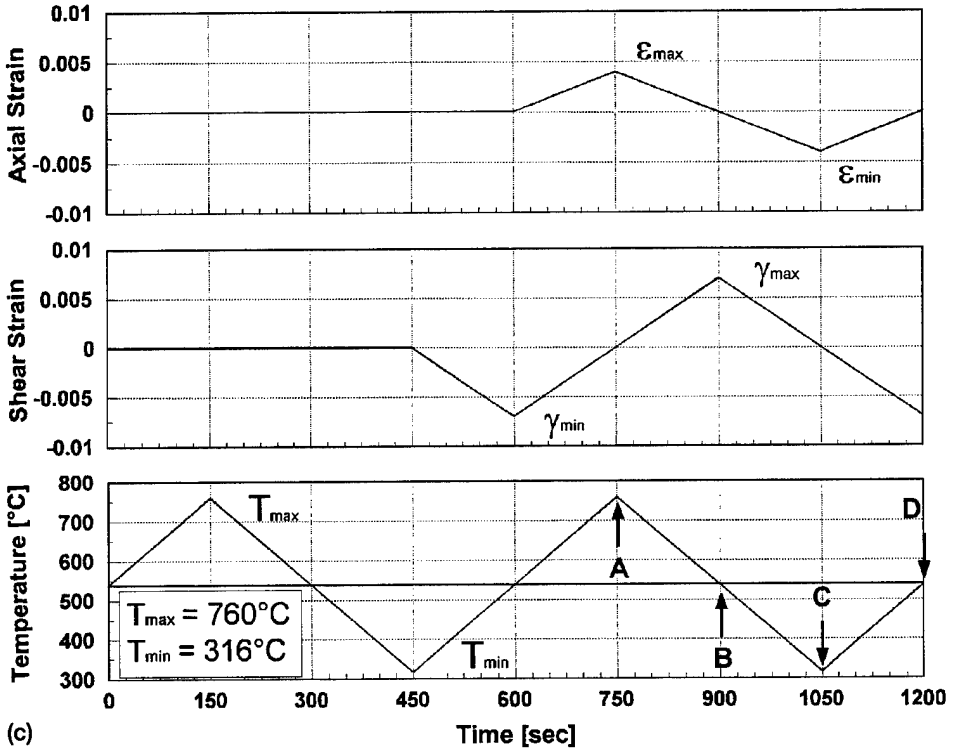

(c)

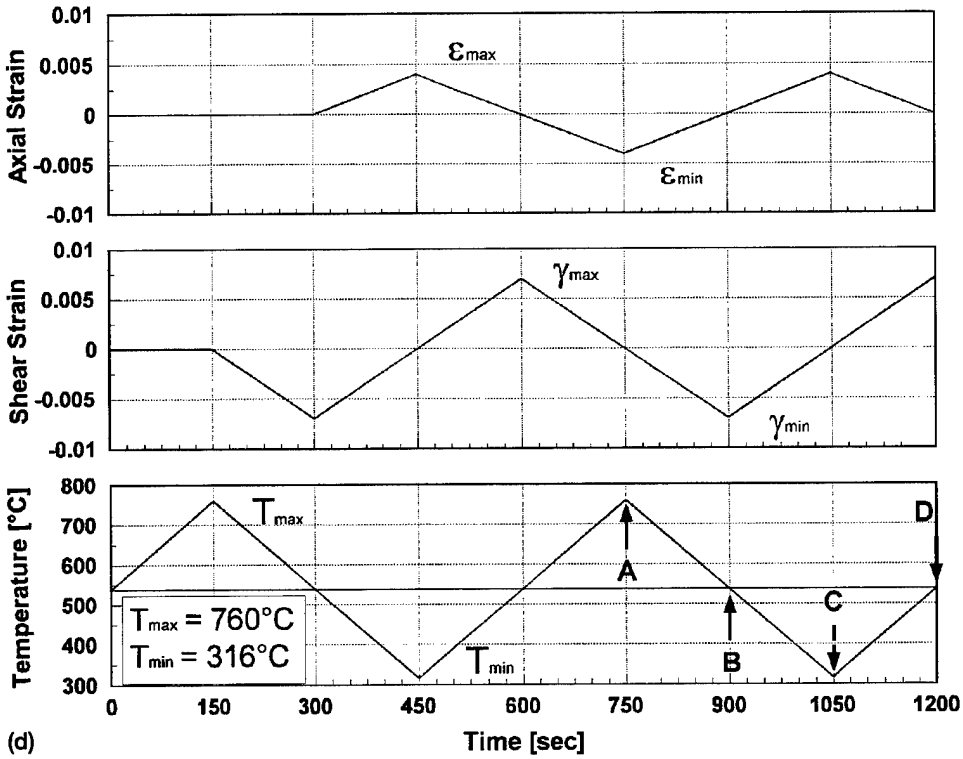

(d)

Figure 1.—Concluded. (c) MOPTIP test. (d) MOPTOP test.

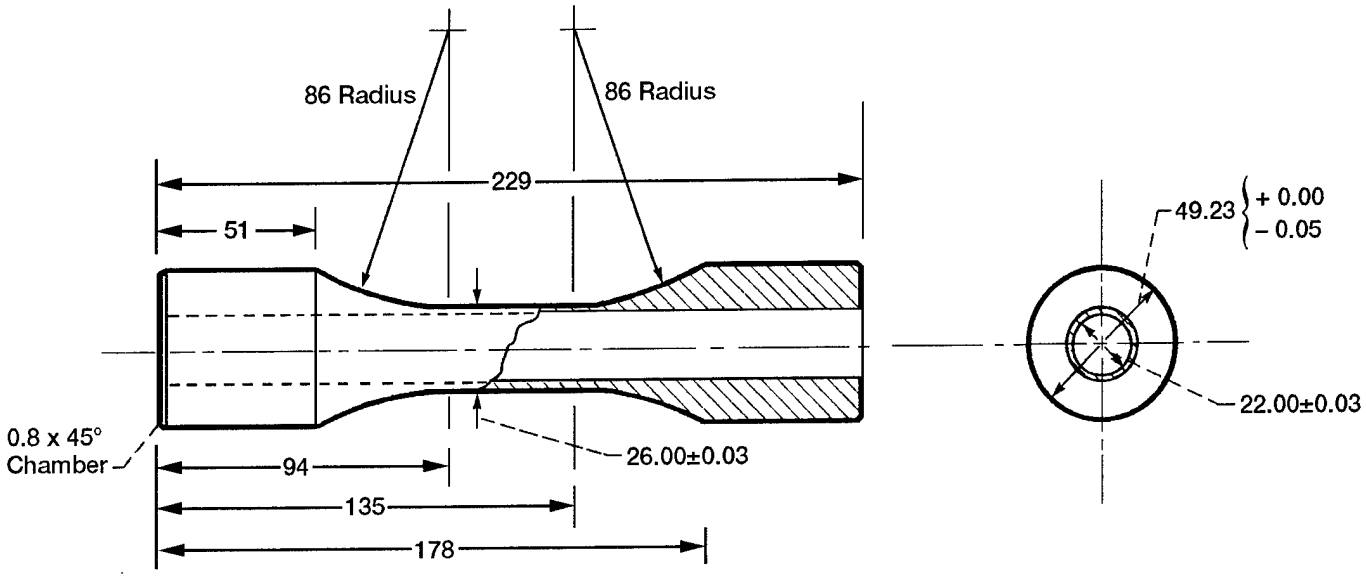

Figure 2.—Schematic of tubular, thin-walled, axial-torsional fatigue specimen. All the dimensions are in mm.

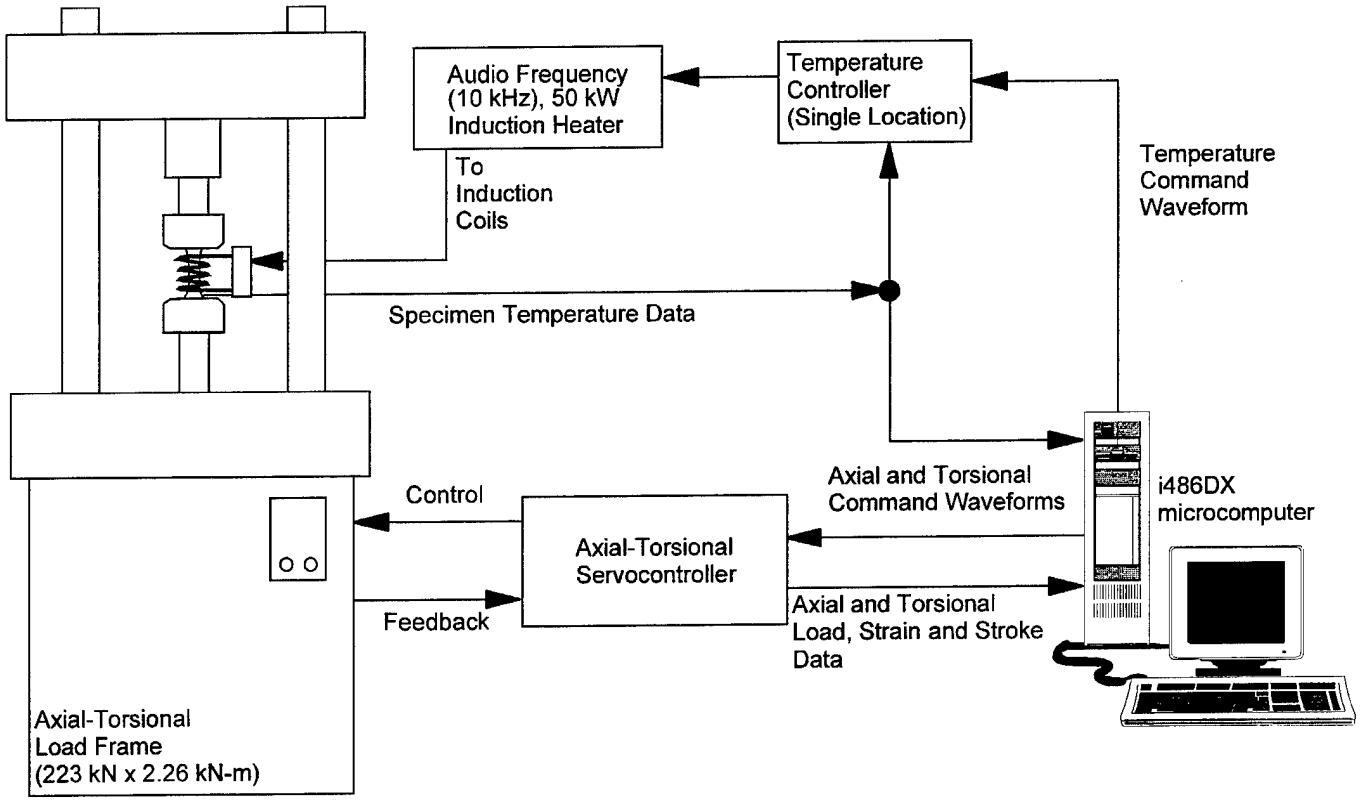

Figure 3.—Schematic of the axial-torsional, thermomechanical fatigue test system.

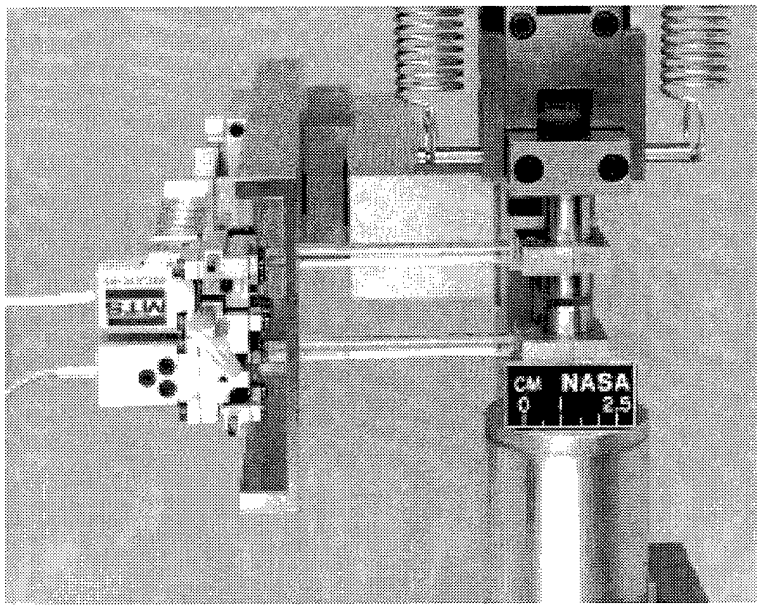

Figure 4.—Axial-torsional extensometer mounted on a calibration fixture.

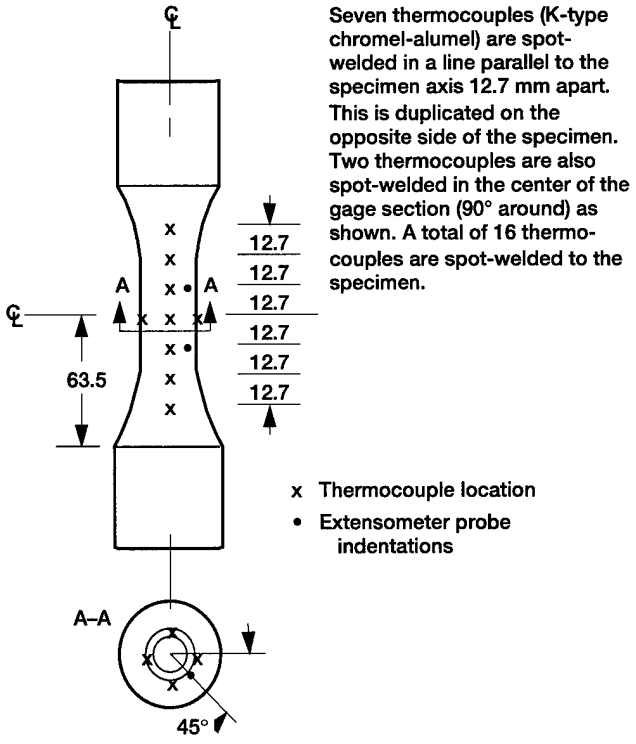

Figure 5.—Schematic of thermocouple layout used for optimizing the induction coil configuration. All the dimensions are in mm.

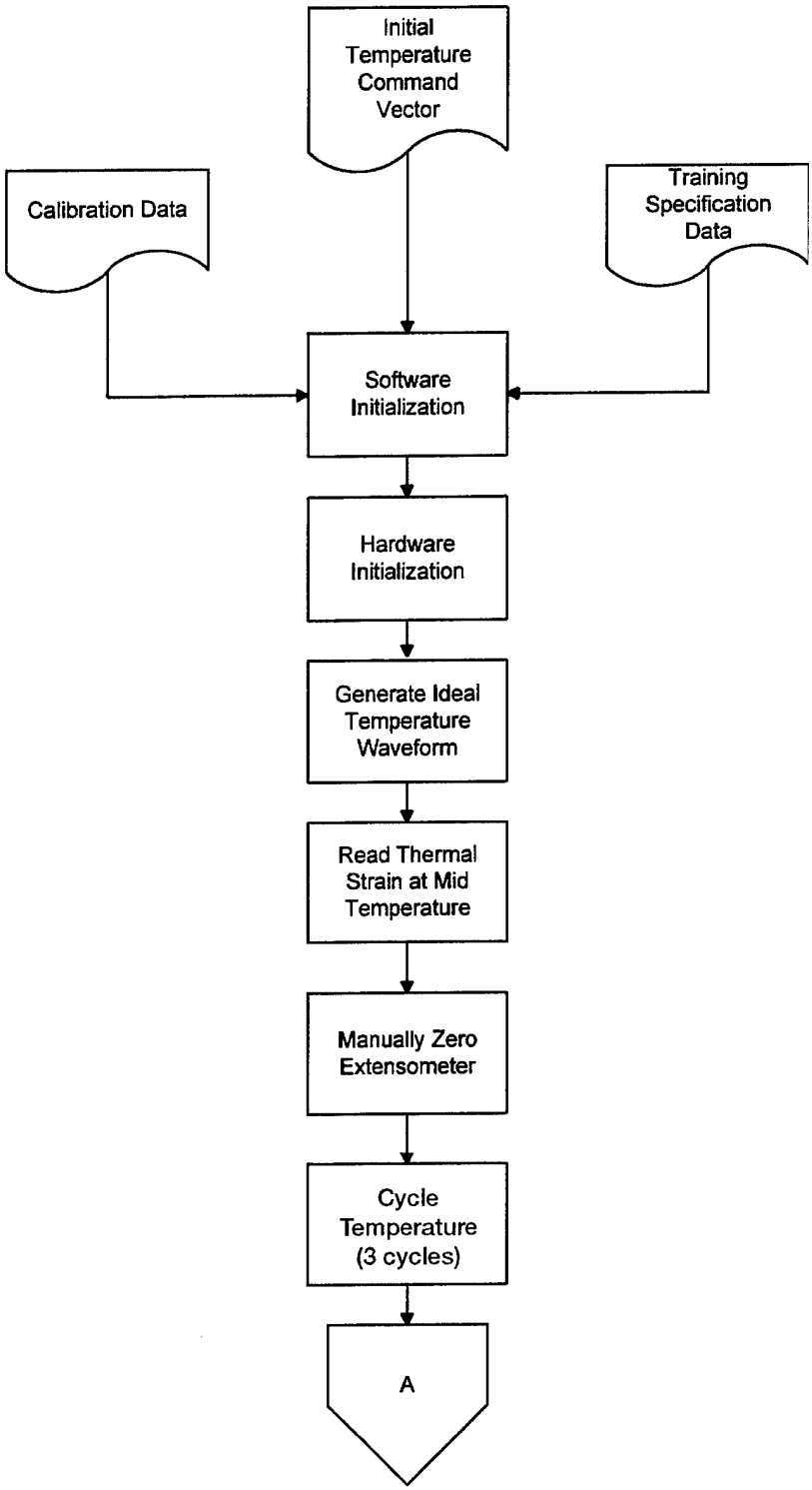

Figure 6.—Flow chart of real-time, successive-correction, training method to obtain remote location temperature control waveform.

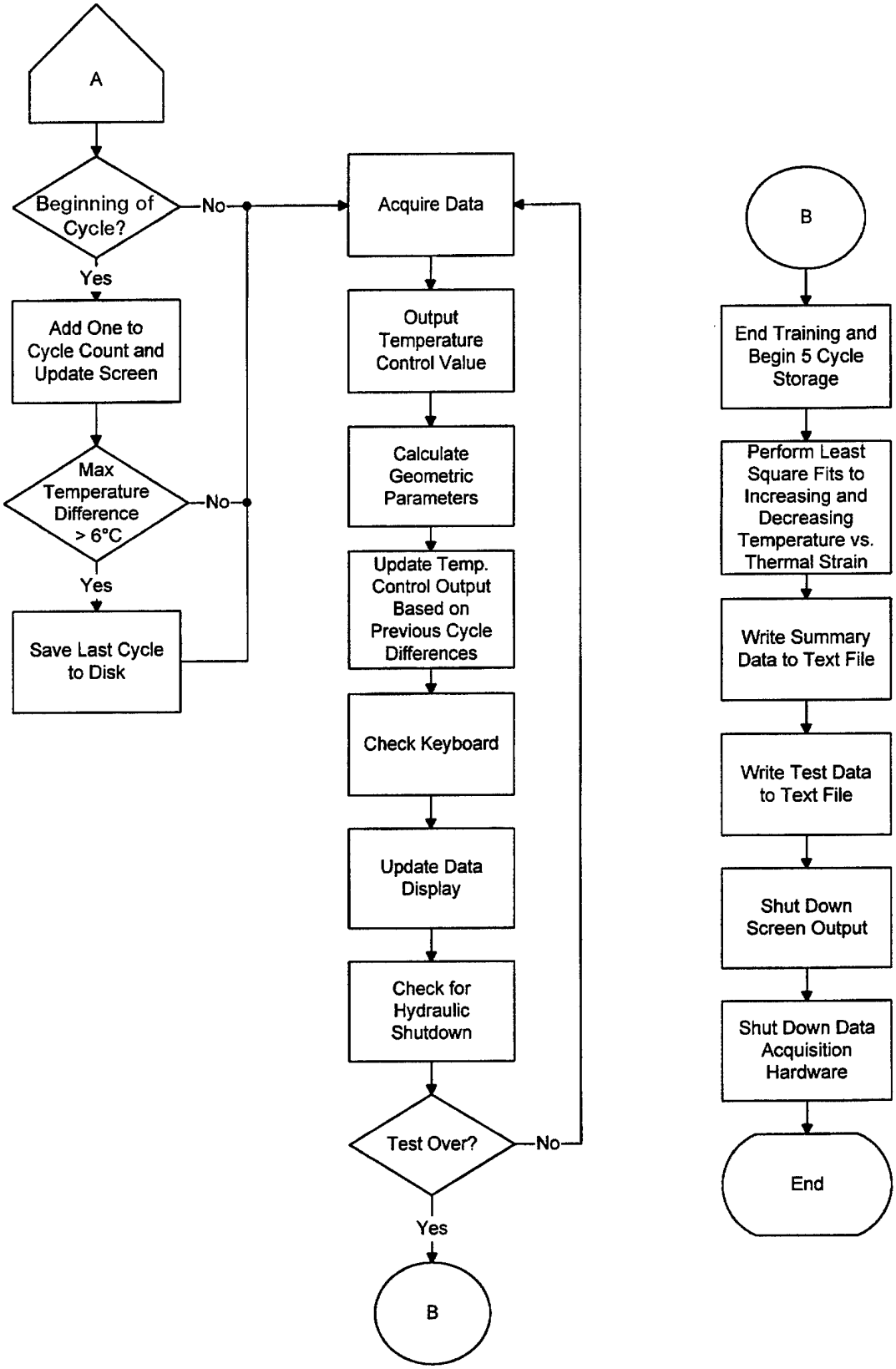

Figure 6.—Concluded.

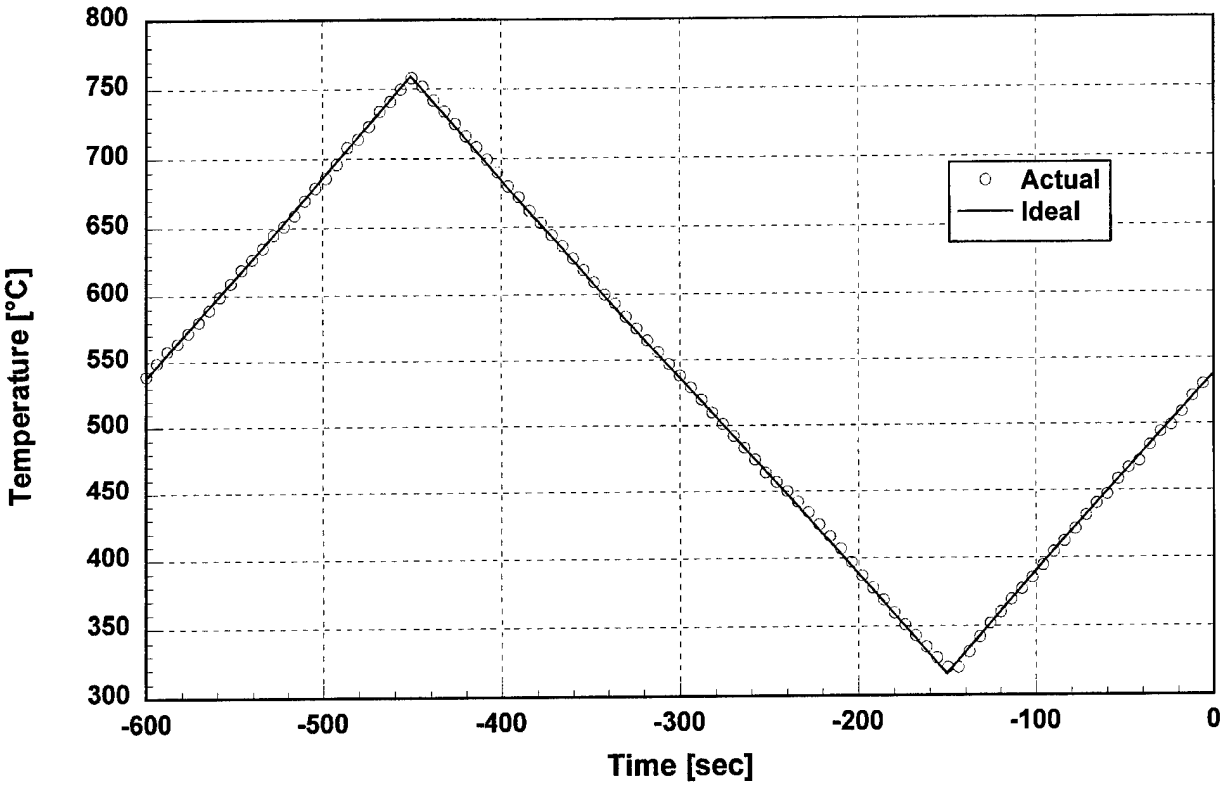

Figure 7.—Gage section temperature waveform obtained after training the remote location temperature waveform.

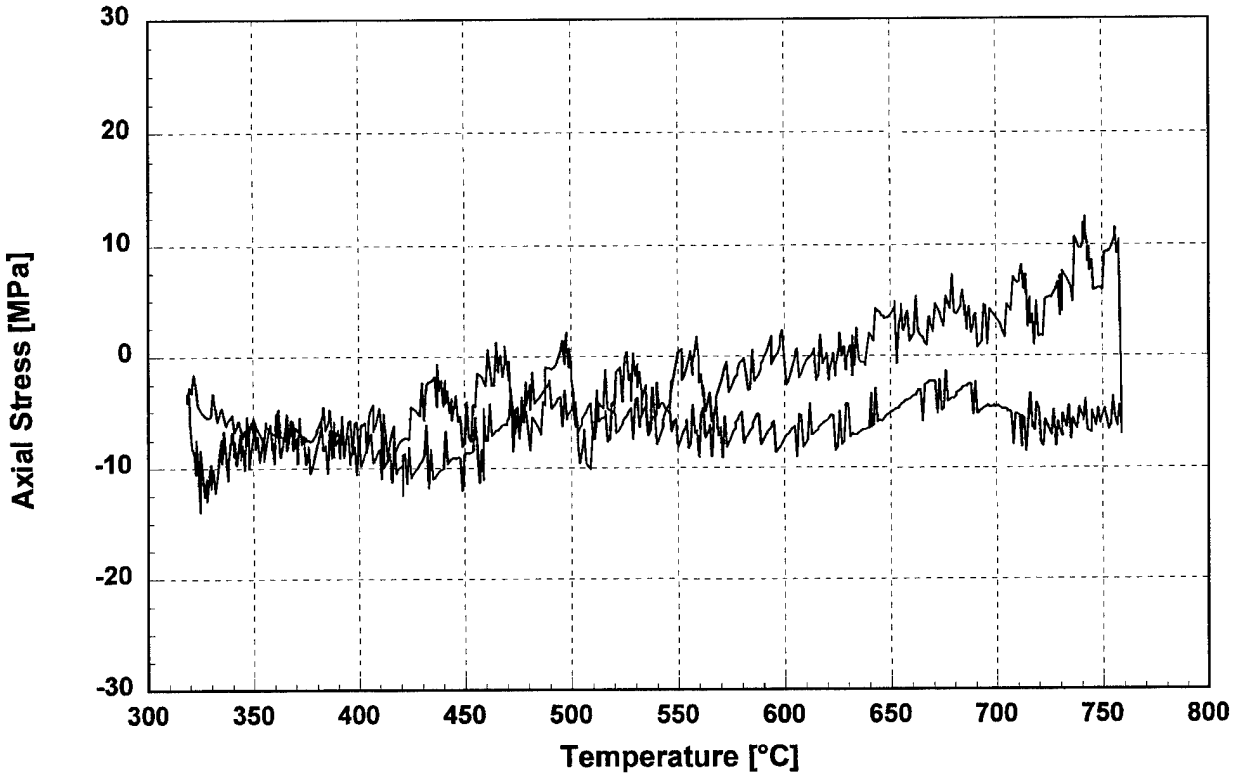

Figure 8.—Largest axial stresses (worst case) developed in one of the AT-TMF tests during a thermal cycle designed to verify thermal strain compensation.

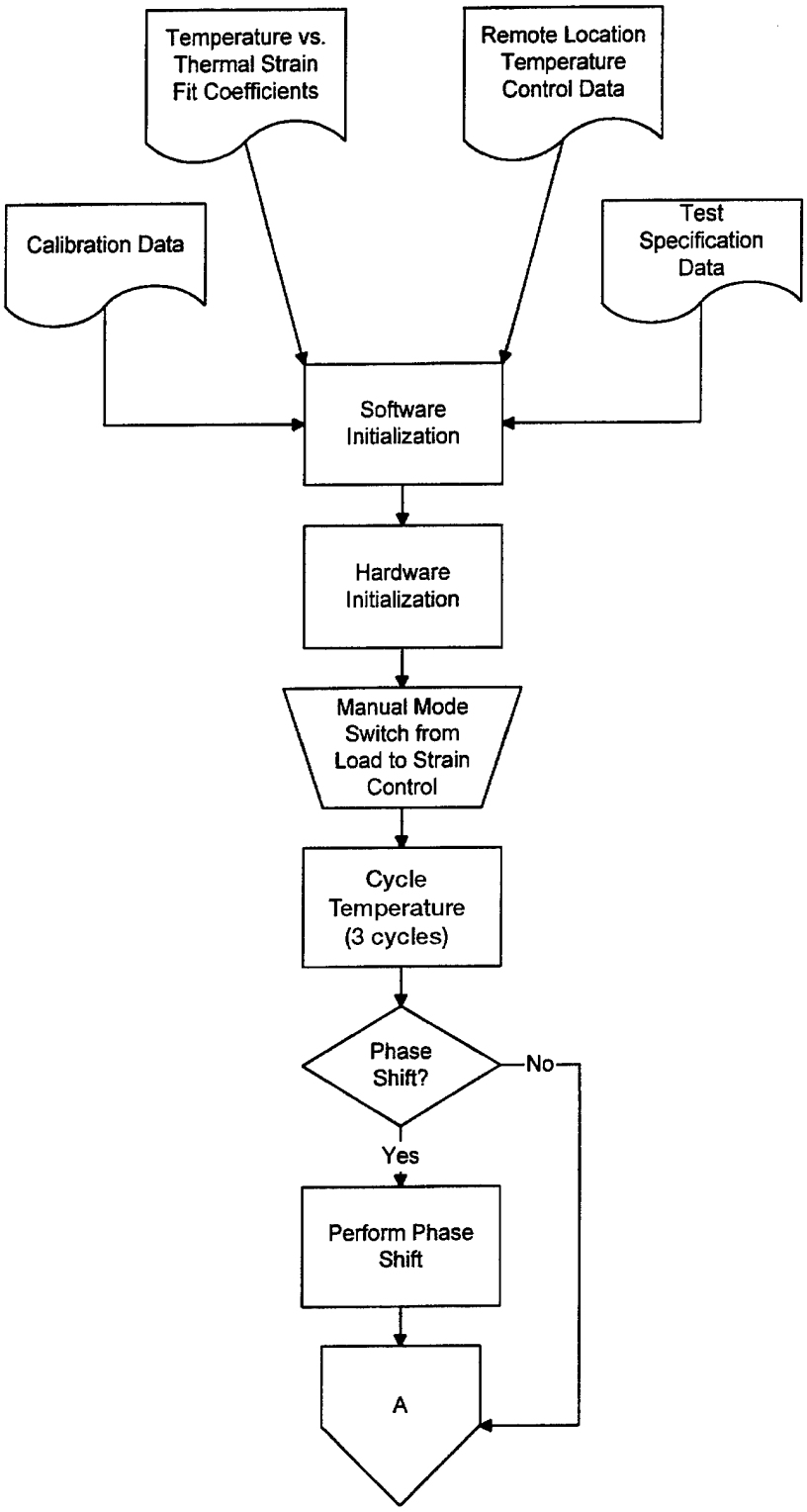

Figure 9.—Flow chart of the procedure for conducting AT-TMF tests.

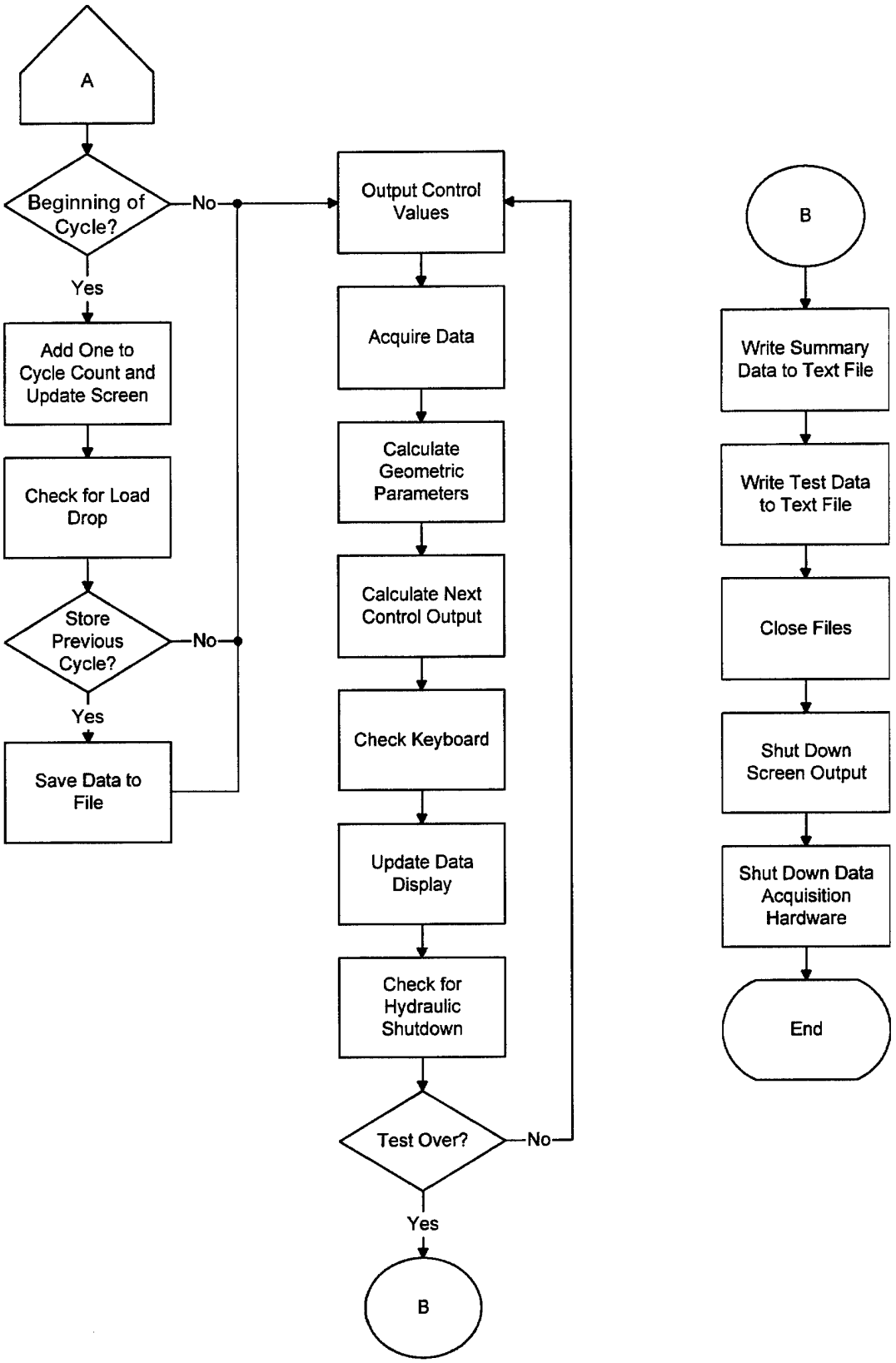

Figure 9.—Concluded.

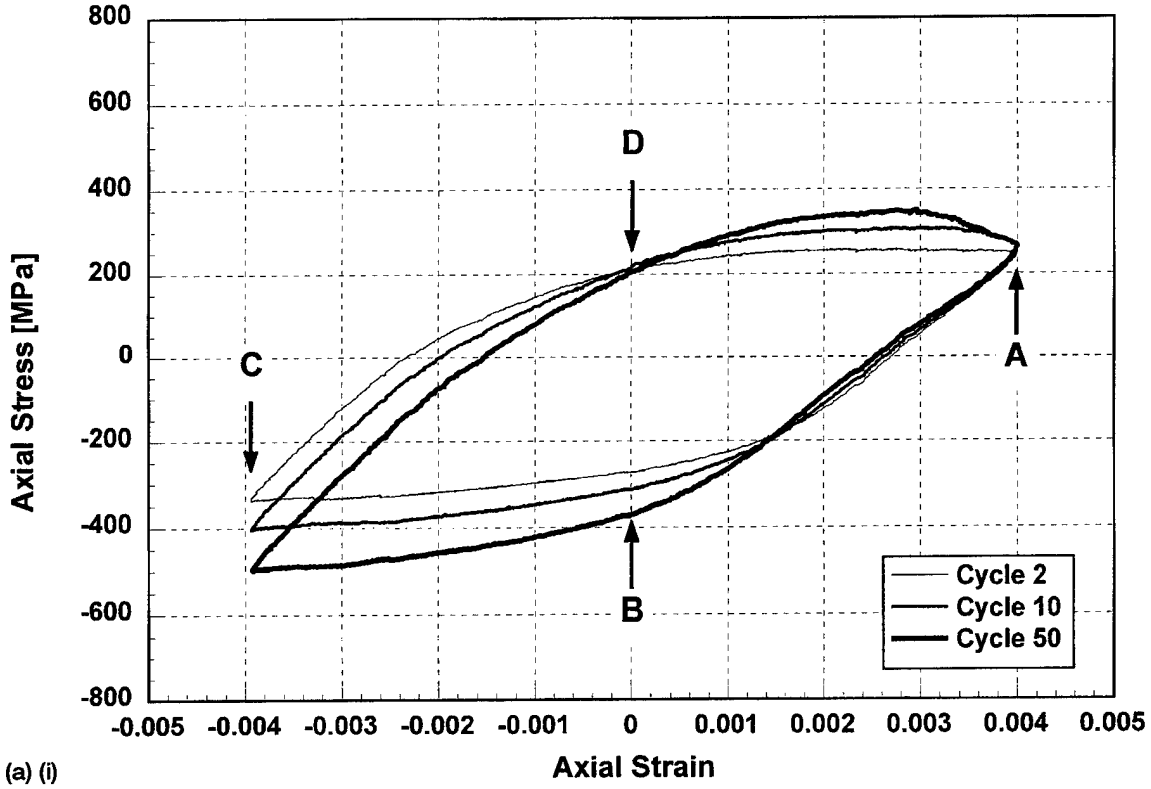

(a) (i)

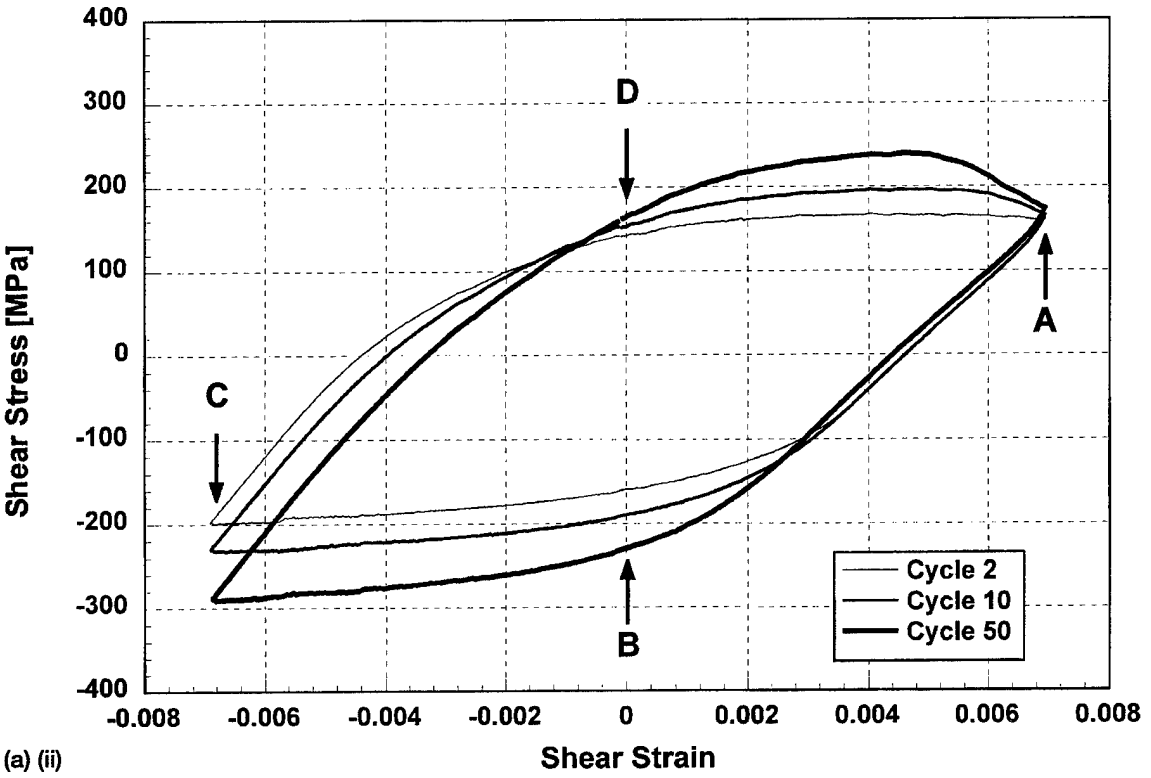

(a) (ii)

Figure 10.—Hysteresis loops generated in the AT-TMF tests. (a) MIPTIP test. (i) Axial hysteresis loops. (ii) Torsional hysteresis loops.

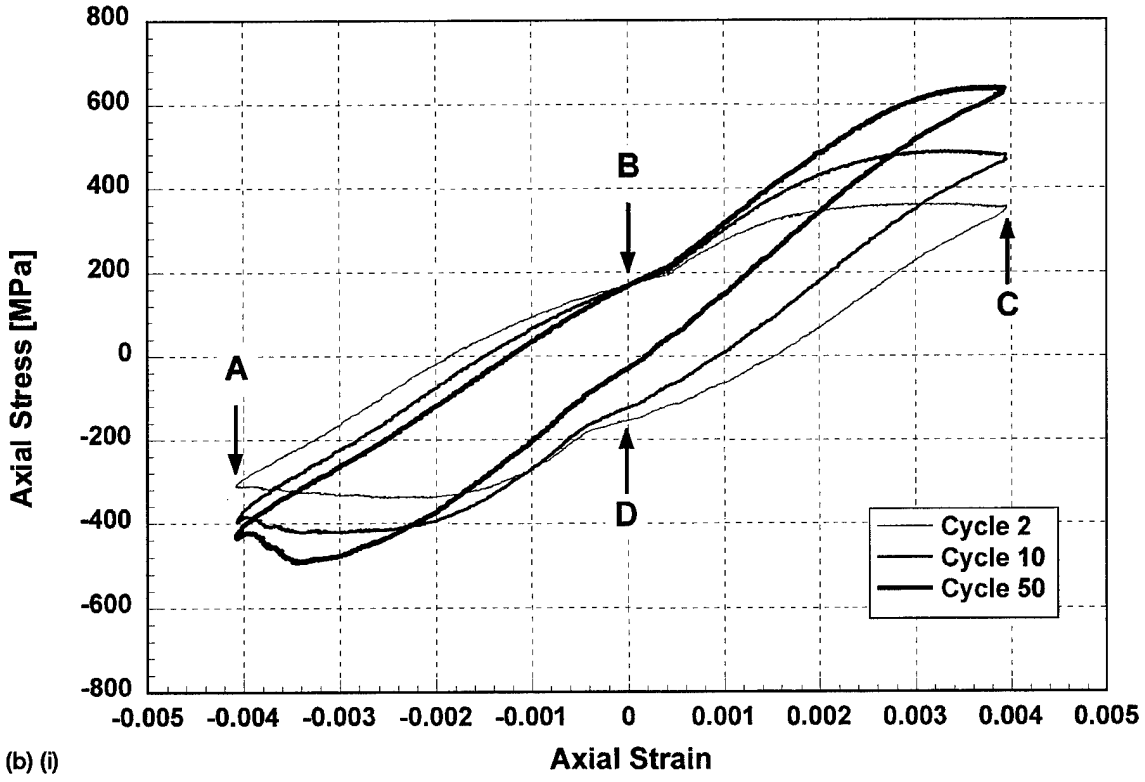

(b) (i)

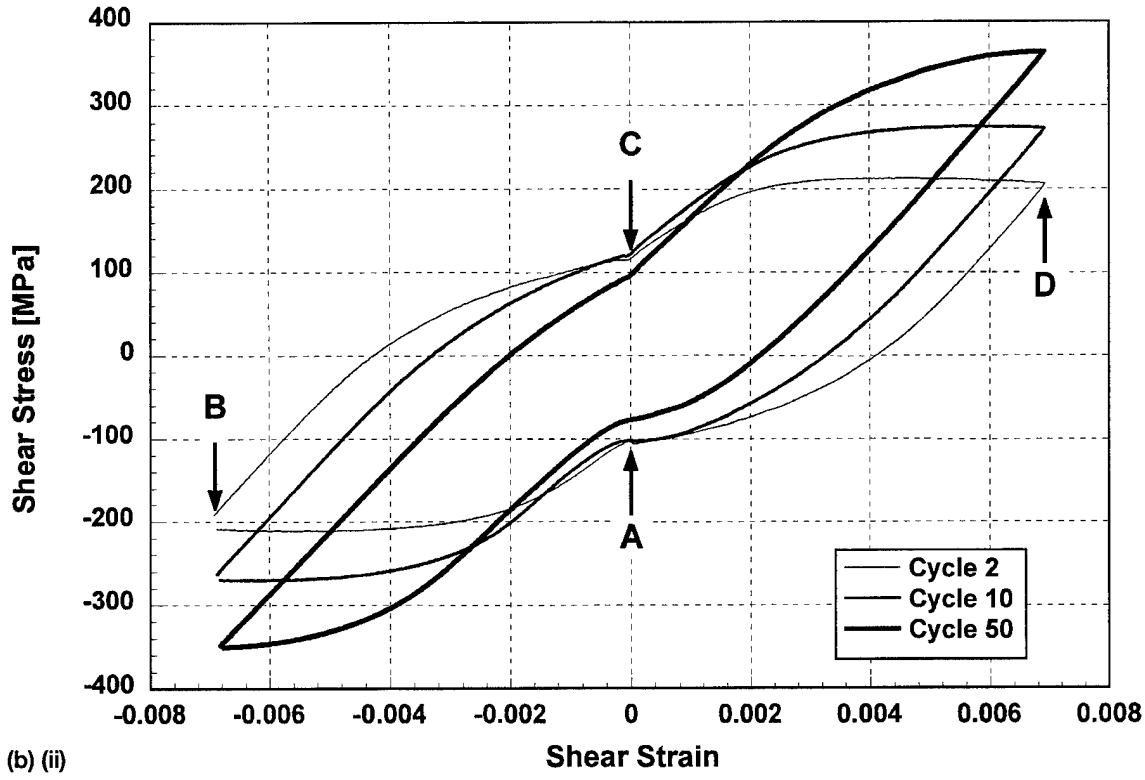

(b) (ii)

Figure 10.—Concluded. (b) MOPTOP test. (i) Axial hysteresis loops. (ii) Torsional hysteresis loops.

$\Delta\varepsilon = 0.008$ **and** $\Delta\gamma = 0.014$

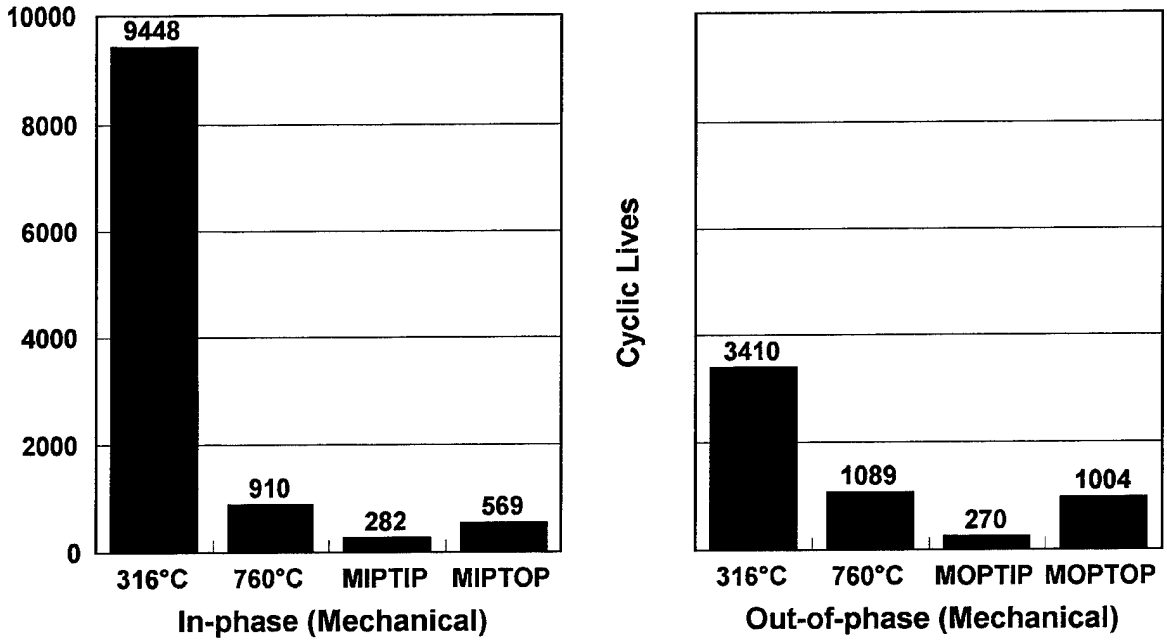

Figure 11.—Comparison of the fatigue lives of isothermal, axial-torsional and AT-TMF tests.

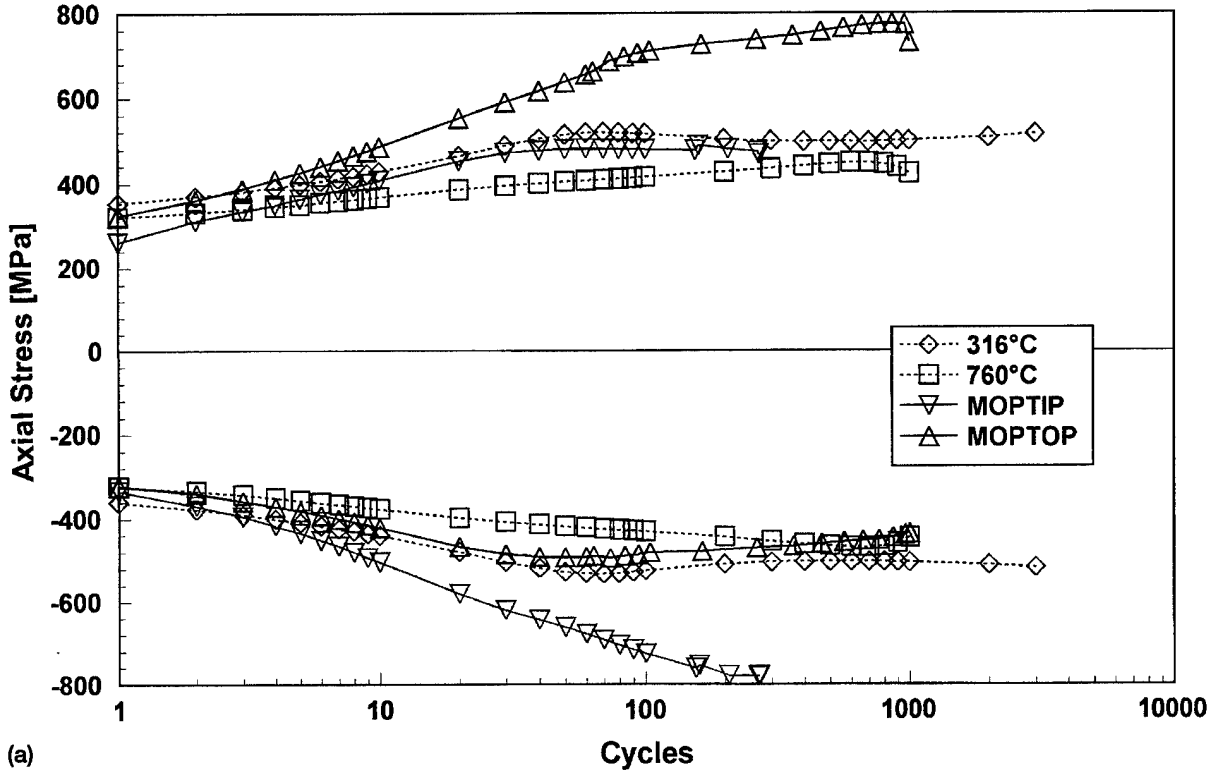

(a)

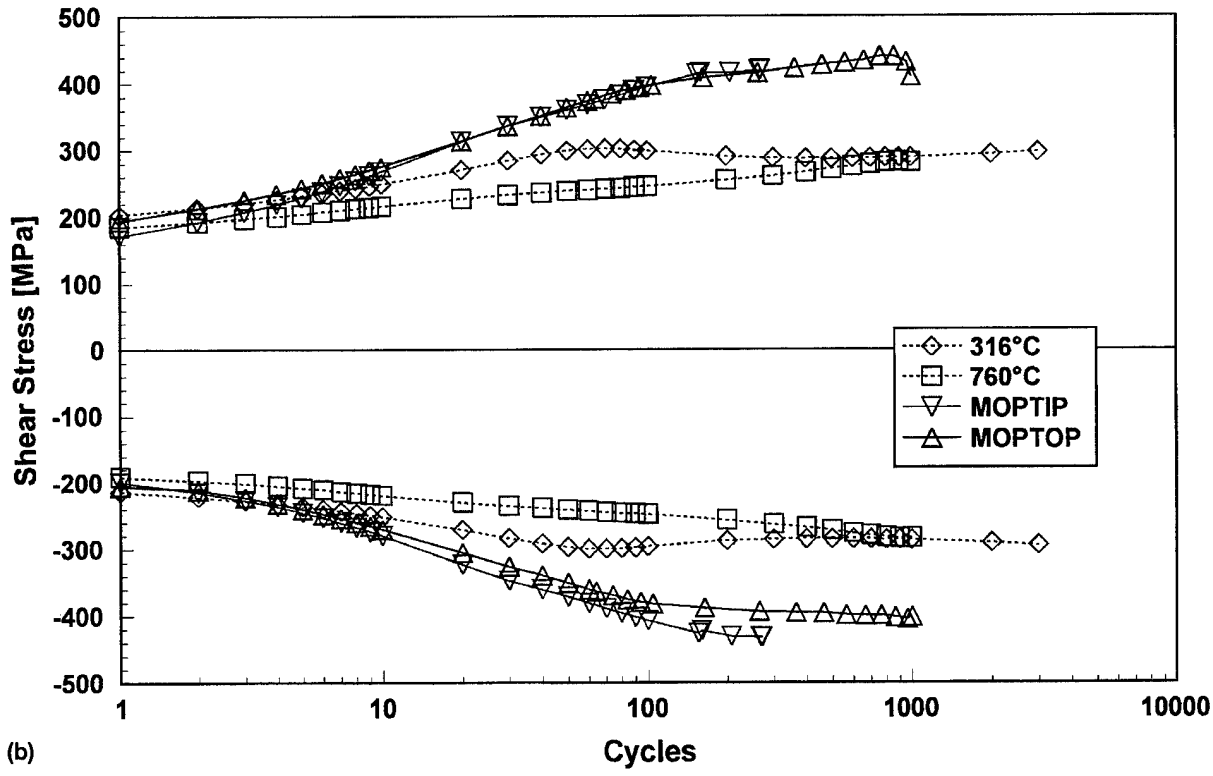

(b)

Figure 12.—Comparison of cyclic hardening in mechanically out-of-phase, isothermal, axial-torsional and AT-TMF tests. (a) Evolution of axial stresses. (b) Evolution of shear stresses.

REPORT DOCUMENTATION PAGE

Form Approved
OMB No. 0704-0188

1. AGENCY USE ONLY (*Leave blank*)	2. REPORT DATE	3. REPORT TYPE AND DATES COVERED
	May 1995	Technical Memorandum

4. TITLE AND SUBTITLE

An Axial-Torsional, Thermomechanical Fatigue Testing Technique

5. FUNDING NUMBERS

WU–505–63–5B

6. AUTHOR(S)

Sreeramesh Kalluri and Peter J. Bonacuse

7. PERFORMING ORGANIZATION NAME(S) AND ADDRESS(ES)

NASA Lewis Research Center
Cleveland, Ohio 44135–3191
and
Vehicle Propulsion Directorate
U.S. Army Research Laboratory
Cleveland, Ohio 44135–3191

8. PERFORMING ORGANIZATION REPORT NUMBER

E–10119

9. SPONSORING/MONITORING AGENCY NAME(S) AND ADDRESS(ES)

National Aeronautics and Space Administration
Washington, D.C. 20546–0001
and
U.S. Army Research Laboratory
Adelphi, Maryland 20783–1145

10. SPONSORING/MONITORING AGENCY REPORT NUMBER

NASA TM–107199
ARL–TR–1060

11. SUPPLEMENTARY NOTES

Prepared for the Symposium on Multiaxial Fatigue and Deformation Testing Techniques sponsored by the American Society for Testing and Materials, Denver, Colorado, May 15, 1995. Sreeramesh Kalluri, NYMA, Inc., 2001 Aerospace Parkway, Brook Park, Ohio 44142 (work funded by NASA Contract NAS3–27186) and Peter J. Bonacuse, Vehicle Propulsion Directorate, U.S. Army Research Laboratory, NASA Lewis Research Center. Responsible person, Sreeramesh Kalluri, organization code 5220, (216) 433–6727.

12a. DISTRIBUTION/AVAILABILITY STATEMENT

Unclassified - Unlimited
Subject Category 39

This publication is available from the NASA Center for AeroSpace Information, (301) 621–0390.

12b. DISTRIBUTION CODE

13. ABSTRACT (*Maximum 200 words*)

A technique for conducting strain-controlled, thermomechanical, axial-torsional fatigue tests on thin-walled tubular specimens was developed. Three waveforms of loading, namely, the axial strain waveform, the engineering shear strain waveform, and the temperature waveform were required in these tests. The phasing relationships between the mechanical strain waveforms and the temperature and axial strain waveforms were used to define a set of four axial-torsional, thermomechanical fatigue (AT-TMF) tests. Real-time test control (3 channels) and data acquisition (a minimum of 7 channels) were performed with a software program written in C language and executed on a personal computer. The AT-TMF testing technique was used to investigate the axial-torsional thermomechanical fatigue behavior of a cobalt-base superalloy, Haynes 188. The maximum and minimum temperatures selected for the AT-TMF tests were 760 and 316°C, respectively. Details of the testing system, calibration of the dynamic temperature profile of the thin-walled tubular specimen, thermal strain compensation technique, and test control and data acquisition schemes, are reported. The isothermal, axial, torsional, and in- and out-of-phase axial-torsional fatigue behaviors of Haynes 188 at 316 and 760°C were characterized in previous investigations. The cyclic deformation and fatigue behaviors of Haynes 188 in AT-TMF tests are compared to the previously reported isothermal axial-torsional behavior of this superalloy at the maximum and minimum temperatures.

14. SUBJECT TERMS

Thermomechanical fatigue; Axial-torsional fatigue; Computer-controlled testing; Data acquisition; Thin-walled tubular specimen; Testing techniques; Hysteresis loop; Cyclic deformation; Cobalt-base superalloy

15. NUMBER OF PAGES

25

16. PRICE CODE

A03

17. SECURITY CLASSIFICATION OF REPORT	18. SECURITY CLASSIFICATION OF THIS PAGE	19. SECURITY CLASSIFICATION OF ABSTRACT	20. LIMITATION OF ABSTRACT
Unclassified	Unclassified	Unclassified	